Efficient third-harmonic generation from visible to deep ultraviolet wavelength in a photonic crystal fiber

JINHUI YUAN[a], XINZHU SANG[a], CHONGXIU YU[a], XIANGWEI SHEN[a], KUIRU WANG[a], BINBIN YAN[a], YING HAN[b], GUIYAO ZHOU[b,c], LANTIAN HOU[b]

[a]*State Key Laboratory of Information Photonics and Optical Communications (Beijing University of Posts and Telecommunications), P.O. Box163 (BUPT), 100876 Beijing, China*

[b]*Institute of Infrared Optical Fibers and Sensors, Physics Department, Yanshan University, 066004 Qinhuangdao, China*

[c]*School of Information and Optoelectronic Science and Engineering, South China Normal University, Guangzhou, 510006*

In the experiment reported here, the initial pump and red-shifted solitons serve as the pump fields, and the third-harmonics in the wavelength range of 288 to 500 nm are efficiently generated based on the phase-matching between the fundamental mode and higher-order modes in a photonic crystal fiber (PCF). When the pump works at 864 nm with the average power of 300 mW, the third-harmonic signals are generated at 288 nm, 320 nm, and 500 nm, the conversion efficiency η_{TH} increases from 0.1% to 1.3%, and the bandwidth B_{TH} changes from 6 to 23 nm. The total efficiency of third-harmonic radiation in the wavelength range of 288 nm to 500 nm, defined as the ratio of the total energy of radiation in the wavelength range of 288 nm to 500 nm to the energy of the input pump, is estimated as 2.2%.

(Received October 15, 2012; accepted February 20, 2013)

Keywords: Photonic crystal fiber (PCF), Initial pump, Red-shifted soliton, Third-harmonic signals

1. Introduction

Third-harmonic generation (THG) is one of the basic nonlinear-optical processes [1], which has been widely used to generate short wavelength radiation for high resolution imaging, direct excitation of electronic molecular transitions, and multiphoton ionization. The advent of photonic crystal fibers (PCFs) [2-4] has opened a new phase in nonlinear optics. Controlled dispersion and enhanced nonlinearity of guided modes provided by PCFs result in a radical enhancement of nonlinear-optical frequency conversion and spectral transformation of laser radiation [5-8]. Efficient THG has been observed in multi-component glass PCFs [9,10]. THG-based PCF sources of short-wavelength radiation have been recently shown to be a powerful tool for studying the time-resolved fluorescence of organic molecules [11]. Femtosecond laser pulses propagating in the anomalous dispersion region in PCFs tend to couple into solitons, which undergo a continuous frequency downshift induced by the Raman effect, called as soliton self-frequency shift (SSFS) [12-16]. The red-shifted solitons can serve as a pump for THG [17]. Some studies have demonstrated the possibility of frequency up-conversion to the short-wavelength region through THG based on the phase-matching between the dispersive-wave THG and the soliton pump [18-20]. However, the THG are mainly concentrated at the visible wavelength, and the conversion efficiencies of pump to third-harmonics are very low. In this paper, the third-harmonics within the wavelength range of 288 to 500 nm are efficiently generated from the input pump field and the red-shifted soliton field at the output of PCF, and the total efficiency of THG can be up to 2.2%, making PCF a multifrequency source from the deep ultraviolet to visible wavelength.

2. PCF properties and experiment

The cross-section of PCF fabricated in our lab is shown in Fig. 1 (a), where the core diameter is 2.6 μm and the relative hole size is 0.83. Fig.1 (b) shows the calculated group velocity dispersion and the effective mode area for the fundamental mode (as shown in inset), where the zero dispersion wavelength is 835 nm, and the value of effective mode area increases from 4.9 to 5.7 μm^2 in the range of 864 to 1500 nm. The effective mode area tends to increase for longer wavelengths because of diffraction, leading to a lower nonlinearity of the PCF in the long-wavelength range.

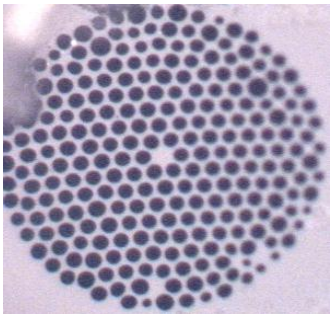

(a)

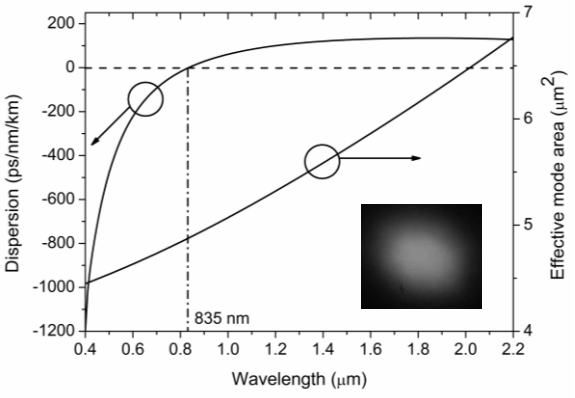

(b)

Fig. 1. (a) The cross-section of PCF used in the experiment. (b) Group-velocity dispersion and effective mode area calculated for the fundamental mode, the vertical dash-line corresponding to the zero dispersion wavelength of 835 nm.

The experimental principle chart is shown in Fig. 2. A mode-locked (Kerr Lens Modelocking, KLM) Ti: sapphire ultrafast laser emitting a pulse train with FWHM of 120 fs (the near transformed limited pulses by compensating the group velocity dispersion) at the repetition rate of 76 MHz is used as the light source. The input power is controlled by a variable attenuator, and an isolator is inserted to block the back-reflection from the input tip of the fiber into the laser cavity. The 40× objective lens with numerical apertures of 0.65 are used for adjusting input and output efficiency, and the CCD1 and CCD2 are used to check the coupling state of input field and observe the output mode field. The fundamental mode can be selectively excited through changing the distance between the input tip of the fiber and the lens to exactly adjust the angle between the input beam and the fiber axis (the offset pumping technique). The optical beam goes through the first split-beam mirror, one part is coupled into the power meter, and the other part is coupled into the PCF span of 50 cm length. The coupling efficiency can be up to 65%. The output spectra of light from the PCF section are monitored by two optical spectrum analyzers (OSA, Avaspec-256 and Avaspec-NIR-256) with the measurement ranges of 200 to 1100 nm and 900 to 2500 nm and the wavelength resolutions of 0.025 nm and 15 nm, respectively.

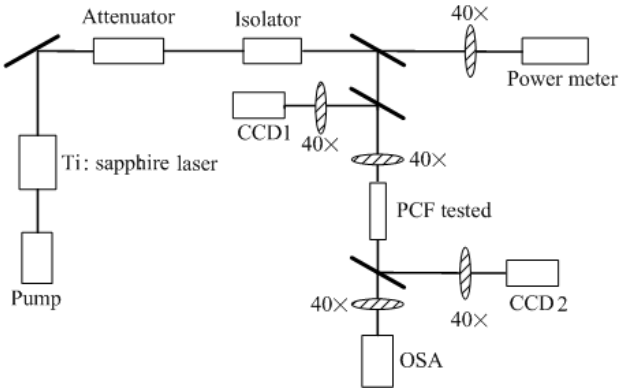

Fig. 2. The experimental principle chart.

3. Results and discussion

The laser pulses tend to form the optical solitons as they propagate through the PCF in the anomalous dispersion region. As shown in Fig. 3 (a), when the pump works at 864 nm with the average power of 300 mW, the input pulse is efficiently coupled into the soliton at 1550 nm, which experiences a wavelength shift exceeding 600 nm within 50 cm PCF due to the Raman effect. The second soliton generated from the residual pump is also observed at 960 nm. The high-order dispersion and the wavelength dependence of the effective mode area tend to reduce the SSFS rate within the long wavelength spectral region.

The third-harmonic can be efficiently generated by laser radiation through the third-order optical nonlinearity of silica material if the phase-matching condition is satisfied. The phase-matching requires the equality of effective mode indices at the pump and third-harmonic frequencies. That is to say, $n_{TH}(3\omega) = n_{sol}(\omega)$, where $n_{TH}(3\omega) = \beta_{TH}(3\omega)c/(3\omega)$ and $n_{sol}(\omega) = \beta_{sol}(\omega)c/\omega$ represent the effective mode indices including the waveguide and material dispersion for the guided modes at the frequencies of the third-harmonic and the pump field, $\beta_{TH}(3\omega)$ and $\beta_{sol}(\omega)$ are the propagation constants of the third-harmonic and the pump, c is the light velocity in vacuum. Here, the initial pump and red-shifted soliton serve as the pump field. As seen from Fig. 3 (b), the third-harmonics are generated at 288 nm (TH3), 320 nm (TH2), and 500 nm (TH1). In Fig. 3 (c), η_{TH} increases from 0.1% to 1.3%, and B_{TH} changes from 6 to 23 nm. The maximum efficiency of THG, defined as the ratio of the total energy of radiation in the wavelength range of 288 to 500 nm to the energy of the input pump, is estimated as 2.2%.

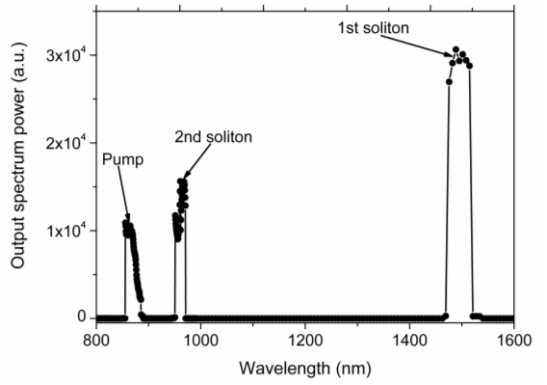

(a)

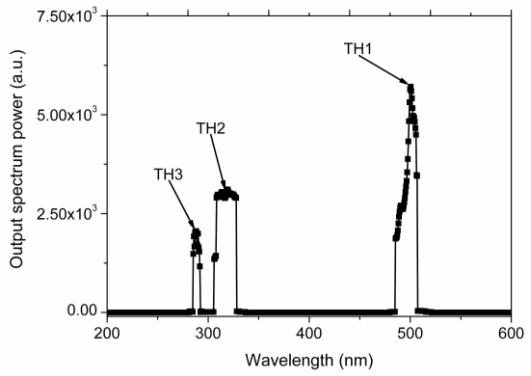

(b)

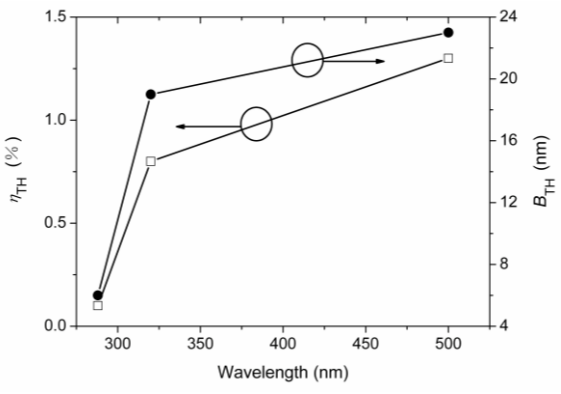

(c)

Fig. 3. (a) The observed output spectrum of pump and soliton when the pump works at 864 nm with the average power of 300 mW, (b) the typical spectrum of the third-harmonic, and (c) the conversion efficiency η_{TH} and bandwidth B_{TH} of third-harmonic as a function of wavelength.

The third-harmonics are generated at different wavelengths, corresponding to several PCF modes simultaneously phase-matched with the fundamental mode for the given regime of nonlinear optical interaction. Thus, the output beam patters are quite complicated because of a mixture of several high-order PCF modes. To study the details of transverse field intensity distribution in the third-harmonics, the fiber is simulated by the supercell plane-wave method, and the material dispersion is included by considering the Sellmeier formula. The calculated transverse field intensity distribution with a six-lobed near-field pattern is shown in Fig. 4 (a). By tilting the fiber axis with respect to the input laser beam, the output spectrum dominated by the emission peak at 320 nm is generated, as shown in Fig. 4 (b). By comparing the simulation result with that of the measured field intensity profile, it can be seen that third-harmonic is generated from the high-order mode due to the modal index of high-order mode propagating at 320 nm being close to that of the fundamental mode at 960 nm.

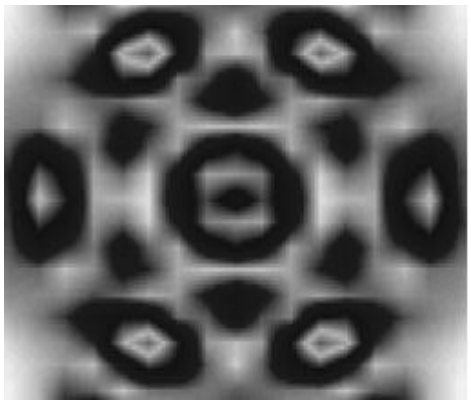

(a)

(b)

Fig. 4. (a) The calculated mode field for λ=320 nm, and (b) the observed far field mode pattern at the output of PCF.

4. Conclusions

In summary, based on the phase-matching between the fundamental mode and high-order modes, the radiations from deep ultraviolet to visible wavelength in PCF are efficiently generated by a combination of Raman SSFS and THG. The total efficiency of THG in the wavelength range of 288 nm to 500 nm is 2.2%. The further work mainly refers to enhancing the THG efficiency through improving the fabrication condition and optimizing the PCF structure parameters to restrain the pulse walk-off and the phase-matching deviations. It can be believed that this multifrequency source from the deep

ultraviolet to visible wavelength will have important applications in the ultrafast photonics and resonant Raman scattering.

Acknowledgements

This work is partly supported by the National Basic Research Program (2010CB327605 and 2010CB328300), the key grant of Ministry of Education (109015), the Program for New Century Excellent Talents in University (NECT-11-0596) and Beijing Nova program (2011066), and the Fundamental Research Funds for the Central Universities (2013RC1202).

References

[1] Y. R. Shen, The Principles of Nonlinear Optics (Wiley, New York, 1984).
[2] P. St. J. Russell, Science **299**, 358 (2003).
[3] J. C. Knight, Nature **424**, 847 (2003).
[4] P. St. J. Russell, J. Lightw. Technol. **24**, 4729 (2006).
[5] J. H. Yuan, X. Z. Sang, C. X. Yu, X. J. Xin, G. Y. Zhou, S. G. Li, L. T. Hou, Optoelectron. Adv. Mater.-Rapid Commun. **4**, 23 (2010).
[6] X. Z. Sang, Y. Wang, J. H. Yuan, C. X. Yu, Q. Zhang, K. R. Wang, X. J. Xin, Optoelectron. Adv. Mater.-Rapid Commun. **4**, 457 (2010).
[7] X. W. Shen, J. H. Yuan, X. Z. Sang, C. X. Yu, L. Rao, M. Xia, C. Lin, Optoelectron. Adv. Mater.-Rapid Commun. **6**, 12 (2012).
[8] J. H. Yuan, X. Z. Sang, C. X. Yu, X. W. Shen, K. R. Wang, B. B. Yan, Y. Han, G. Y. Zhou, L. T. Hou, Electron. Lett. **48**, 1150 (2012).
[9] A. N. Naumov, A. B. Fedotov, A. M. Zheltikov, V. V. Yakovlev, L. A. Mel'nikov, V. I. Beloglazov, N. B. Skibina, A. V. Shcherbakov, J. Opt. Soc. Am. B **19**, 2183 (2002).
[10] E. E. Serebryannikov, A. B. Fedotov, A. M. Zheltikov, A. A. Ivanov, M. V. Alfimov, V. I. Beloglazov, N. B. Skibina, D. V. Skryabin, A. V. Yulin, J. C. Knight, J. Opt. Soc. Am. B **23**, 1975 (2006).
[11] S. Konorov, A. Ivanov, D. Ivanov, M. Alfimov, A. Zheltikov, Opt. Express **13**, 5682 (2005).
[12] N. Nishizawa, T. Goto, IEEE J. Sel. Topics Quantum Electron. **7**, 518 (2001).
[13] X. Liu, C. Xu, W. H. Knox, J. K. Chandalia, B. J. Eggleton, S. G. Kosinski, R. S.Windeler, Opt. Lett. **26**, 358 (2001).
[14] N. Ishii, C. Y. Teisset, S. Köhler, E. E. Serebryannikov, T. Fuji, T. Metzger, F. Krausz, A. Baltuška, A. M. Zheltikov, Phys. Rev. E **74**, 036617-1 (2006).
[15] J. H. Yuan, X. Z. Sang, C. X. Yu, K. R. Wang, B. B. Yan, X. W. Shen, Y. Han, G. Y. Zhou, S. G. Li, L. T. Hou, IEEE Photon. Technol. Lett. **24**, 670 (2012).
[16] J. H. Yuan, X. Z. Sang, C. X. Yu, Y. Han, G. Y. Zhou, S. G. Li, L. T. Hou, IEEE Photon. Technol. Lett. **23**, 786 (2011).
[17] F. G. Omenetto, A. J. Taylor, M. D. Moores, J. Arriaga, J. C. Knight, W. J. Wadsworth, P. St. J. Russell, Opt. Lett. **26**, 1158 (2001).
[18] A. Yulin, D. V. Skryabin, P. St. J. Russell, Opt. Lett. **29**, 2411 (2004).
[19] A. A. Ivanov, D. Lorenc, I. Bugar, F. Uherek, E. E. Serebryannikov, S. O. Konorov, M. V. Alfimov, D. Chorvat, A. M. Zheltikov, Phys. Rev. E **73**, 016610-1 (2006).
[20] A. B. Fedotov, A. A. Voronin, E. E. Serebryannikov, I. V. Fedotov, A. V. Mitrofanov, A. A. Ivanov, D. A. Sidorov-Biryukov, A. M. Zheltikov, Phys. Rev. E **75**, 016614-1 (2007).

*Corresponding author: yuanjinhui81@163.com